Color Ultrasound Image Watermarking Scheme Using FRT and Hessenberg Decomposition for Telemedicine Applications

Lalan Kumar

(School of Computing, Graphic Era Hill University, Dehradun, India
https://orcid.org/0000-0003-3037-5383, lalankumar100@gmail.com)

Kamred Udham Singh

(Department of Computer Science and Information Engineering, National Cheng Kung University, Taiwan,
School of Computing, Graphic Era Hill University, Dehradun, India
https://orcid.org/ 0000-0002-7201-6381, kamredudhamsingh@gmail.com)

Abstract: Watermarking is a valuable technique for verifying medical images obtained through the internet for diagnosis. There is a greater need for security in medical pictures with ever-increasing security risks. This research presented a Finite Ridgelet Transform (FRT)-Hessenberg based watermarking scheme in medical images. The suggested paradigm is divided into two stages. Before watermark insertion, FRT is applied to medical images. The coefficients are combined into blocks of 4 x 4 and each block is decomposed using Hessenberg decomposition. The second column of the Q matrix is used to insert the watermark using the additive quantization technique. The results obtained from our experiment have given good visual quality of the watermarked images. The high PSNR value 53.6121 and NC value 1.0 show that our scheme is performing better. Moreover, the performance of our scheme is robust against several attacks. The consequences of this result imply that the anticipated scheme is effective for medical image watermarking.

1 Introduction

The watermark insertion domain is connected to many watermarking methods available in the literature, such as multiresolution, spatial, frequential, etc. Each representation has several performance settings [Shehab et al. 2018], [Singh et al., 2022(a)]. The selection of watermarking is a decisive step in expanding watermarking systems. In the spatial domain, embeddings of watermarks are carried out by reliably altering the values of every pixel. The elementary benefit of this field is that embedding and extraction processes are computationally economical. Therefore, it can be used in real-time watermarking applications [Liu et al. 2018]. The main drawback is that the human perceptual quality declines after embedding. Moreover, these approaches are subject to attack.

In the frequency domain, the watermarks are kept in the transformed domain instead of spatial [Singh et al. 2018], [Singh and Singhal 2018]. To get the frequency

representation of the image, a Discrete Fourier Transform (DFT) or a Discrete Cosine Transform (DCT) is used [Zainol et al. 2020]. The key parts of these schemes are to select the major coefficients. The solution for achieving a robust and invisible watermarked image is to insert the watermark into the frequency position. The watermark could be entrenched into the middle frequency to increase perceptual quality while reducing the opportunity of the watermark to get rid of by compression or noise addition when located in high frequencies [Thanki et al. 2019]. Regardless of the inherent advantage of domain, translation and scale invariance, this approach is computationally costly and sensitive to local deformation [Liu et al. 2019]. It can be characterized by image subbranding, which allows low-frequency components to be segregated, resulting in a less sensitive insertion zone [Araghi and Manaf 2019]. Once a multiresolution translation, the spatial content of the image is preserved, and the information may be used to find a watermark after a geometric change. Spatial and Transform domains are two groups of image watermarking techniques. The watermarks are directly placed into the cover image [Tan et al. 2019]. They are advantageous because of their simplicity and ease of implementation, but they are typically sensitive to geometrical assaults. DFT [Molina-Garcia et al. 2020], DCT Wavelet transform are examples of transform domain watermarking approaches [Araghi et al. 2018]. These approaches enable more data to be encoded and give higher attack resistance, but they necessitate more labour overall. Several hybrid approaches have been proposed based on Hessenberg decomposition and other transforms [Golub et al. 1979]. Although it suffers from FPP (false positive issue), embedding in the Q matrix is preferred in Hessenberg decomposition due to its stability and capacity to survive assault [Hou et al. 2019]. Watermarking techniques have been proposed to solve FPP [Sadreazami and Amini 2018]. The FPP, on the other hand, cannot be entirely avoided in this manner.

The proposed work is an FRT and Hessenberg [Golub et al. 1979] based system for medical image watermarking to increase performance. The created watermark model analyses the input medical image after performing FRT and Hessenberg putrefaction by taking frequency bands into account. The blocks are shuffled using random numbers. A secrete key is used to produce random numbers to entrench watermarked images successfully. The proposed FRT and Hessenberg performance is evaluated in a variety of attack situations, including noise and scale assaults.

This paper is organized as follows: Part II portrays the overview of the watermarking scheme. Section III explains the anticipated research approach for the embedding and extraction process of the watermarking method. Section IV introduces a method for watermarking, followed by the findings achieved with the suggested system. Section VI concludes with the general conclusion.

2   Related Work

The watermark insertion domain is connected to several image watermarking methods available in the literature, such as spatial, frequential, multi-resolution, etc. Every image representation region offers many performance possibilities.

The embedding domain is an important stage in developing watermarking systems. The fundamental advantage of this domain is that embedding & detection processes are computationally inexpensive and allow it to be exercised in real-time watermarking applications [Zheng and Zhang 2020]. Spatial domain embedding is carried out by

directly amending the pixel values. The most significant disadvantage is that the image's visual quality declines after integration. Furthermore, these approaches are subject to assault. The watermarks are implanted into the transformed domain rather than the image in frequency domain insertion. A DFT or DCT is used to calculate the frequency representation of the picture [Ahmadi et al. 2021]. The most challenging component of this method is selecting the recommended coefficents. The best strategies for achieving a suitable robustness-invisibility compromise frequently place the mark in the image's middle frequency to maximize imperceptibility while minimizing the possibility of the watermark being detached by compression or noise addition if placed in high frequencies [Meenakshi et al. 2020].

In [Wang et al. 2020], a hybrid watermarking approach has been proposed that utilizes visual cryptography with watermarking (VCW). A VCW is exercised to segment images as well as to determine the smallest energy band in which the watermarks are included for the integration of a watermark communicating the medical image owner's information [Golub et al. 1979]. Anand and colleagues proposed a method for embedding several watermarks in medical images. The embedding watermark is made of text as well as images. To boost safety, the watermarked images are ciphered using the hyperchaotic ciphering algorithm. The work proposed in [Rakhmawati et al. 2019] recommended a blind watermarking method which employs both DWT and SVD. The watermarked images are disordered using Arnold Transform for security. Homomorphic transform & Arnold transform are all proposed by Zhong et al. in [Zhong et al. 2020]. Following that, the watermark bits are embedded into the resultant unique values.

In [Elhadad et al. 2021], a watermarking scheme for DICOM images has been proposed. This method's three key components are preprocessing embedding based, DCT, and extraction. They employ MRI, PSNR, MSE, SSIM, UQI, and the correlation coefficient. The author offered a mechanism in [Malayil and Vedhanayagam 2021] for measuring the adaptive validation codes from a watermarked picture. This watermarked image is fused with the medical image by means of a unique image proportioning approach. Although proportioning real image to M × M pixels through a factor of 2, the original pixel values must be used to estimate the amount of pixel strengths in the proportionate image. By duplicating the neighbour pixels as MPI values, a set of policies is developed to integrate the validation code as well as EPR data in the resultant scaled-up image. A window-based method was advised for ROI the recognition of MRI brain images through eliminating high-density salt and pepper noise was proposed in [Ebrahimnejad and Naghsh 2021]. This scheme focuses on improving the watermarking technology's resilience and invisibility to avoid medical conflicts. Based on a considerable variation in CAT (Cellular Automata Transform), the medical picture watermarking approach was developed for copyright protection [Qasim et al. 2019]. To get two low-frequency bandwidths, the medical pictures are first subsampled into four sub- pictures, out of them two are selected at random. MSI (Master share image) is created by extracting essential elements from suspicious medical images. The authors of [Fan et al. 2019] presented the Fourier transform colour image watermarking scheme.

The FFT transformation is employed on each of the colour components of an image. The resultant coefficient parity is used with the watermark to cover up it in the middle frequency range. For DICOM, security-based ciphering and watermarking approach was formulated. It provides data privacy, integrity, and validation based on a

reversible watermark. The sender-side integrity is accomplished through extracting the hash value-based ciphering MD5 from the image. The Huffman compression technique is employed to compress the image and R–S Vector is elicited from the image to retain the reversible quality. [Abd-Eldayem 2013] described a cryptographic solution for maintaining the secrecy and integrity of DICOM images. AES and Blake Hash Function are two cryptographic algorithms that are employed. In [Navamani et al. 2019], they suggested a blind, fragile, and ROI lossless MIW approach that may be used as an all-in-one solution tool for a range of medical data distribution and management difficulties, including security, secure archiving, and authentication.

2.1 Finite Ridgelet Transform

There are two-step processes to calculate the finite ridge let transform (FRIT): discrete Radon transform computation, and a wavelet transform. Two steps calculate the finite radon transform (FRAT): In the Radon projection of an image, a function of one-dimensional inverse FFT and a two-dimensional FFT is applied to all its 32 radials. In the three layers of putrefaction, a one-dimensional wavelet is employed, restricted to radial direction temporarily through the origin. To accomplish FRAT, a series of projections are used for the representation of images acquired from different angles to map the image space to projection space. The computation is vital to process as well as computer vision and pattern detection & reconstruction of DICOM images, on a finite grid is defined by FRAT real function. The Radon projection is calculated by signifying the set points to build up a line on lattice. For one every pixel in the row, the original image's pixels might be transferred and the histogram. Lastly, the histogram values are divided such that the mean values can be computed. The Ridgelet transform is straightforward as stated by Alzubi in [Alzubi et al. 2011], after the wavelet and radon transforms are used. Before reaching the output multiplier, every Radon projection output is only sent through the wavelet transform.

2.2 Hessenberg Decomposition

The factorization of a nonspecific matrix M into the form of Hessenberg putrefaction is the factorization of a nonspecific matrix M into the form of orthogonal similarity transformations [Golub et al. 1979].

$$M = QHQ^T$$

When i > j + 1, h_{ij} = 0 since Q is an orthogonal matrix and H is an upper Hessenberg matrix. Householder matrices are usually used to achieve Hessenberg putrefaction. The Householder matrix (P) is a kind of orthogonal matrix.

$$P = \frac{I_n - 2uu^T}{u^T u}$$

where u in R^n is a vector of nonzero and is an identity matrix of size n x n. When n x n is the size of A, the total process has n-2 steps. As a result, the following is how Hessenberg decomposition is calculated:

$$H = (P_1 P_2 \dots P_{n-3} P_{n-2})^T A (P_1 P_2 \dots P_{n-3} P_{n-2})$$

$$H = Q^T A Q$$
$$A = Q H Q^T$$

where $Q = P_1 P_2 \ldots P_{n-3} P_{n-2}$.

3   Proposed Scheme

The foundation of the proposed method of watermarking is based on hybridization of FRT along with Hessenberg putrefaction. The proposed watermarking method is non-blind and robust against several attacks. The FRT transforms an image into double the size of the real image. Let P, x Q be the size of an image. The FRT transformed coefficients of the image can be 2 P x 2 Q. Since, it augments the payload capacity of the watermarking scheme; therefore, the double size watermark can be entrenched into the half-size host image. However, the Hessenberg decomposition factorizes a generic matrix M into the form of orthogonal similarity transformations as described in Section 3.2. The individual colour components are greyscale, and the pixel value ranges from 0 to 255. If the block of a pixel is putrefactive using Hessenberg putrefaction, then there are trivial alters in the orthogonal matrix. The elements of the succeeding columns in the unitary matrix are much alike. In other words, there is a slight dissimilarity between any two elements in the matrix Q. The slight alteration in the subsequent column can improve the invisibleness and robustness of the watermark. Thus, the blended uses of FRT and Hessenberg putrefaction are used in the proposed method to accomplish robust watermarking and high payload scheme.

To accomplish better perceptual quality and robust (against image processing attacks) watermarked image; the watermark should be entrenched in a protected manner such that it can be recovered with possible image processing attacks. Therefore, frequency domain transforms are extensively used for image watermarking. The watermark embedding method is discussed in Section 4.1 and the extraction process is discussed in Section 4.2.

3.1 Watermark Embedding Process

In this subsection, the watermark embedding procedure is being discussed. The diagram for the anticipated watermark entrenched system is illustrated in Figure 1. In the first step, the FRT is employed on host medical image in which the watermark is to be entrenched and transform coefficients are obtained. A single dimensional vector is used to represent the watermark and the secret key is used to shuffle the elements. The watermark image is also ciphered with the same secrete key. In the second step, blocks of 4 x 4 are created with the coefficients obtained in the previous step. Another secrete key is used to randomly shuffle the blocks. The shuffling of blocks guarantees the robustness of the watermarking system. In the third step, Hessenberg putrefaction is employed on every block to get the orthogonal matrix Q in which the watermark bits are being embedded. The column two of Q matrix is used to entrench the watermark bits since the elements of column two of the orthogonal matrix are much alike. In step four, the column two of Q matrix is used to quantize the watermark bits. The equation to quantize the watermark bits is given in step 5 of the embedding algorithm. In the

fifth step, an inverse Hessenberg putrefaction is performed, and the blocks are reshuffled using the secrete key. Finally, the watermarked image is gained by employing inverse FRT.

In the proposed watermarking method, the watermark is embedded into the green channel of the host image. The algorithm to embed the watermark is given as follows.

Algorithm 1:
Input: Host medical image and watermark image
Output: watermarked image

Step 1: Let a host image (HI) and a watermark image (WI).
Step 2: Perform FRT on HI to get Ridgelet transform coefficients. Renovate the watermark image (WI) into a one-dimensional vector. The vector is randomly shuffled.
Step 3: The FRT coefficients are further converted into nonoverlapping blocks of 4 x 4 and are randomly shuffled.
Step 4: Hessenberg putrefaction is applied on each block to get Q matrix.
Step 5: The watermark bits are quantized into Q matrix using Equation 4.

$$Q' = \begin{cases} q(x,1) + \alpha, & if \ w = 1 \\ q(x,1) + 0, & if \ w = 0 \end{cases}$$

Step 6: Perform inverse Hessenberg decomposition and reshuffle the blocks.
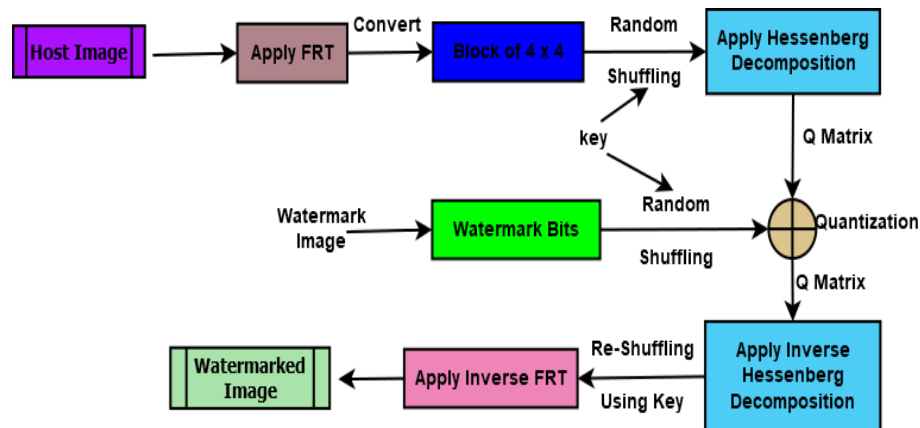Step 7: Perform Inverse FRT to obtain the watermarked image.

Figure 1: Block diagram for the watermark embedding process

3.2 Watermark Extraction Process

In this subsection, the procedure of extraction the watermark is explained. In Figure 2, the illustrates the watermark recovery process and the algorithm to extract the watermark is given in Algorithm 2.

To recover the watermark, firstly the watermarked image is transformed using FRT. Then the coefficients of FRT are converted into blocks of 4 x 4. Afterwards, these blocks are randomly shuffled using the secrete key used in the embedding process. Hessenberg putrefaction is employed on each block to obtain Q matrix. The watermark bits are extracted using the equation derived in step 5 of the extraction algorithm and the threshold value α is utilized to recover the watermark bits. The extracted watermark bits are reshuffled to get the watermark.

Algorithm 2
Input: watermarked image
Output: Extracted watermark

Step 1: Take a watermarked image (WI).
Step 2: Perform finite Ridgelet transform (FRT) WI to obtain Ridgelet transform coefficients.
Step 3: The FRT coefficients are further converted into blocks of 4 x 4 and are randomly shuffled.
Step 4: Hessenberg putrefaction is applied on each block to get Q matrix.
Step 5: Inverse quantized is performed on Q matrix to obtain the watermark bits using Equation 5.

$$W' = \begin{cases} 1, & if\ q(x,1) - \alpha \geq t \\ 0, & otherwise \end{cases}$$

Step 6: Watermark bits are reshuffled to extract the watermark image.
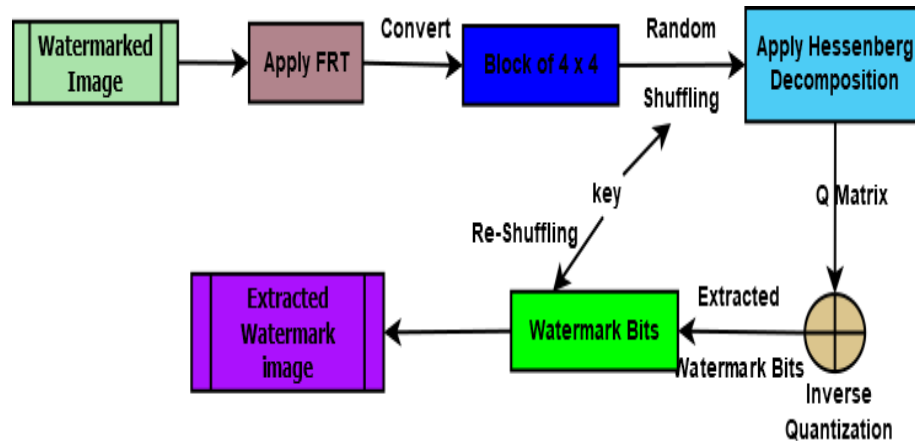

Figure 2: Block diagram for extraction process

4   Experimental Setup

This section gives a detailed overview of our experimental setup of watermarking and extraction process of the proposed scheme. In our experiment, colour medical images of ultrasound have been used which is shown in Figure 3, available in the public domain

[Liu et al. 2020]. In Figure 3a – 3f, the image of ultrasound of a patient is shown. The bitmap watermark image used in our experimentation is shown in Figure 3g. The experimental ultrasound image size is 255 x 255. The patient information is intentionally removed for security reasons. The experiment was conducted on Intel core-i7 processor with 8 GB RAM using MATLAB. The green channel of the colour medical image has been used to entrench the watermark. The effectiveness of the anticipated method is assessed by various quality measures such as PSNR, NCVC, NCPR, NC. These parameters show the quality, performance, and robustness of any scheme. The detailed discussion on these parameters has been discussed further in this section.
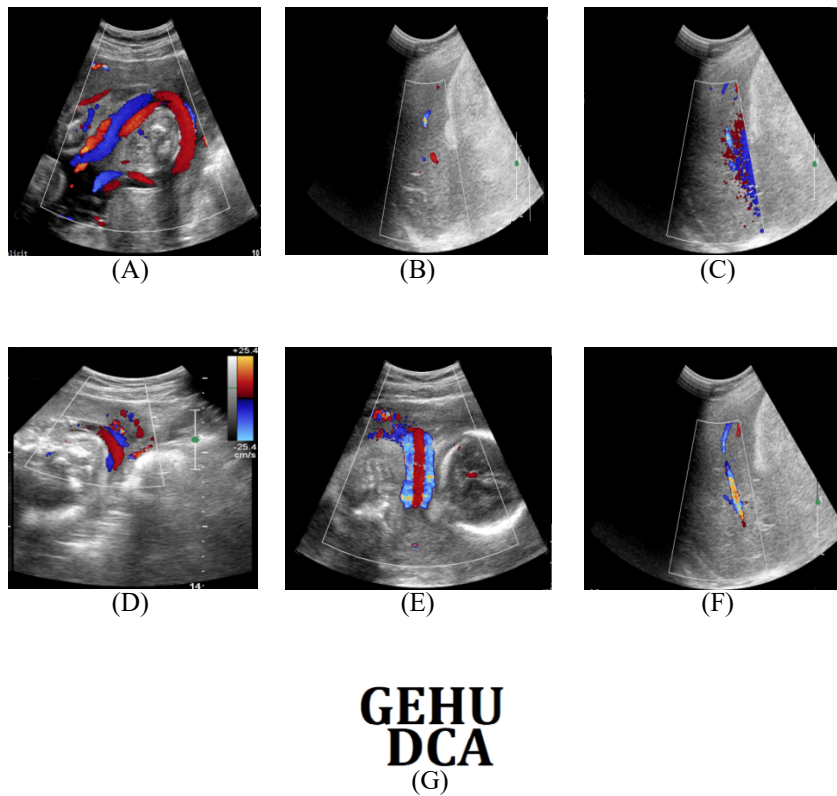

(A)   (B)   (C)

(D)   (E)   (F)

(G)

Figure 3: Ultrasound Images Used in our Experiment

The parameters such as Peak signal-to--to-noise ratio (PSNR) and Normalized Correlation (NC) are useful to assess the effectiveness of the scheme [Najafi and Loukhaoukha 2019], [Singh et al. 2022(b)]. PSNR is concerned with evaluating the degradation of dB with the entrenching process in the watermarked images using the following equation.

$$PSNR_{dB} = 10\log_{10}\left[M*N\frac{\max^2(i,j)}{\sum i,j[l(i,j)-J(i,j)]^2}\right]$$

An image ratio of change in the number of pixels with respect to the integration process (NPCR) is provided for the computation of the original and watermarked images which are calculated using the following equation.

$$NPCR = \sum_{i=1}^{M}\sum_{j=1}^{N}\frac{D(i,j)}{T}*100$$

$$D(i,j) = \begin{cases} 0, & \text{if } Cl_1(i,j) = Cl_2(i,j) \\ 1, & \text{if } Cl_1(i,j) \neq CI_2(i,j) \end{cases}$$

The number of colorimetric values changed is exploited to establish how many colorimetric values were changed throughout the integration process. It is computed by comparing the values of the colour components (Red, green, and Blue) of the original and watermarked images (P and Q), as shown in the equation

$$\text{NCVC} \equiv \sum_{i=1}^{M}\sum_{j=1}^{N}(P_r(i,j)-Q_r(i,j))\pm\left(P_g(i,j)=Q_g(i,j)\right)$$
$$+(Q_b(i,j)-Q_b(i,j))$$

Structural Similarity of the image computes the visual quality and compare with the original and compressed images [Singh et al. 2022(c)]. The discrepancy between two images is assessed on pixel-to-pixel. The equation of SSIM is as follows

$$SSIM(x,y) = \frac{\left(2\mu_x\mu_y + C_1\right)\left(2\delta_{xy}+C_2\right)}{\left(\mu_x^2+\mu_y^2+C_1\right)\left(\delta_x^2+\delta_y^2+C_2\right)}$$

Unified averaged changed intensity is computed as follows

$$UACI = \sum_{i=1}^{M}\sum_{j=1}^{N}\frac{CI_1(i,j)-CI_2(i,j)}{F*T}*100$$

5   Results and Discussion

This section discusses the investigated consequences of the anticipated work having been examined. There are diverse types of ultrasound medical images that have been used in our experiment, as shown in Figure 3. The patient's information has been removed from the ultrasound medical images. This section also discusses the effects of different quality measures and results obtained during our experiments. Table 1 shows PSNR, NC, NPCR, UACI, and the average of NPCR & UACI of ultrasound medical images after watermarking process.

Image Name	PSNR	NC	NPCR	UACI	Avg. of NPCR & UACI
A	53.6121	1.0000	0.8184	0.2811	0.5498
B	52.9137	0.9705	0.9448	0.3444	0.6442

C	52.8187	0.9509	0.9801	0.3463	0.6632
D	51.7483	1.0000	0.8451	0.3079	0.5765
E	51.6567	0.9478	0.8628	0.3214	0.5921
F	52.6801	0.9898	0.9101	0.3313	0.6207
Average value	52.5716	0.9765	0.8935	0.3220	0.6077

Table 1: Performance of proposed scheme on various medical images

The PSNR value obtained during the experiment ranges from 51-53dB for six different ultrasound images. The obtained PSNR values suggest that the goodness of our system is good in terms of perceptibility of the watermarked images. The high PSNR shows a low gain factor. The NC values obtained in our results ranging from 0.94 to 1.00, tabulated in Table 1, exhibiting that the anticipated method has a high gain factor, the perceptual quality of the watermarked image. The PSNR of watermarked images are greater than 51 dB and the maximum NC value (i.e., 1.0). The NPCR value ranges from 0.81 to 0.98 shows the computation between original and watermarked images. The image ratio of change in terms of pixel values in the embedding process. Unified averaged changing intensity of watermarked images shows the intensity of changes during the embedding process. In our case, the changing intensity is low. The range of UACI is 0.28 to 0.34 approximately. Moreover, the overall quality parameters on to which the performances are being evaluated in terms of visual/perceptual quality show better results. Therefore, we can assert that the anticipated scheme performs better while entrenching the bitmap watermark image into the host colour ultrasound medical images.

Attack	PSNR	SSIM	Extracted Watermark
Median	33.0584	0.89486	
Salt and pepper noise	34.8129	0.99981	

Speckle noise	40.2979	0.9769	GEHU DCA
JPEG Compression	35.8799	0.8839	GEHU DCA
JPEG2000 Compression	35.6636	0.88908	GEHU DCA
Sharpening attack	33.2972	0.98055	GEHU DCA
Histogram equalization	8.0702	0.20172	GEHU DCA
Average Filter	33.9385	0.88983	GEHU DCA
Gaussian low-pass filter	46.7819	0.99916	GEHU DCA

Motion blur	28.1801	0.78149	GEHU DCA
Gaussian noise	31.6272	0.78771	GEHU DCA

Table 2: PSNR and SSIM after various attacks

The effectiveness of the anticipated watermark extraction scheme is assessed by performing an experiment on a watermarked ultrasound medical images. We have used diverse image processing attacks to assess the performance in terms of the robustness of our watermarking scheme as well as the robustness of the watermark extraction process of our scheme. Table 2 exhibits the resultant PSNR of the watermarked images and SSIM of the extracted watermark after different attacks carried on the watermarked images. The strength of attack was 0.04 and 0.06. The attacks can distort the imperceptibility of the image. The PSNR values of watermarked image after median filter attack is 33.0584, Salt & pepper noise is 34.8129, Speckle noise is 40.2979, JPEG Compression is 35.8799, JPEG2000 compression is 35.6636, Sharpening attack is 33.2972, Histogram equalization is 8.0702, Average Filter is 33.9385, Gaussian low-pass filter is 46.7819, Motion blur is 28.1801, and Gaussian noise is 31.6272. These values show that how attacks distort the perceptual quality of images. The perceptual quality of the extracted watermarks has been found much better after employing attacks on the watermarked images.

The SSIM value ranged from 0.78 to 0.97 as exhibited in table 2. The SSIM values of extracted watermark after median filter attack is 08948, Salt & pepper noise is 0.9998, Speckle noise is 0.9769, JPEG Compression is 0.8839, JPEG2000 compression is 0.8890, Sharpening attack is 0.9805, Histogram equalization is 0.2017, Average Filter is 0.8898, Gaussian low-pass filter is 0.9991, Motion blur is 0.7814, and Gaussian noise is 0.7877. The SSIM values of the extracted watermark images confirm that the resistance of the watermarked image against attacks. The SSIM values portray that the anticipated scheme performed better under various types of image attacks.

Attacks	Gain Factor	Noise Density	[Thanki et al. 2019]	[Thakur et al. 2019]	Proposed scheme
Salt & Pepper Noise	0.7 0.9	0.04 0.06	0.9736 0.9646	0.9734 0.9641	1.0 0.9798

Gaussian Noise	0.7	0.04	0.9849	0.9841	1.0
	0.9	0.06	0.9888	0.9872	1.0
Speckle Noise	0.7	0.04	0.9522	0.9496	0.9656
	0.9	0.06	0.9285	0.9275	0.9898

Table 3: Comparison of NC Values attacks

We have assessed the NC values of the anticipated scheme with several existing schemes shown in Table 3. The assessment was evaluated based on the attacks used during the experiment. The strength of attack was 0.04 and 0.06 and the gain factor was 0.7 and 0.9. The NC values obtained by [Thanki et al. 2019] and [Thakur et al. 2019] were 0.9736, 0.9646, 0.9734 & 0.9641 respectively whereas in the proposed scheme it is 1.0 & 0.9798 in salt and pepper attack. In Gaussian attack, NC values of the proposed scheme were 1.0 & 1.0, whereas the NC values of [Thanki et al. 2019] and [Thakur et al. 2019] were 0.9849, 0.9888, 0.9841 and 0.9872 respectively. Similarly, we have obtained NC value 0.9656, 0.9898 by applying Speckle noise attack & [Thanki et al. 2019] and [Thakur et al. 2019] have shown 0.9522, 0.9285, 0.9496 & 0.9275 respectively.

Based on the above results and assessments, we have drawn the consequence that the performance of the extraction process of the watermark is higher than existing watermarking schemes.

Comparison parameter	[Thakur et al. 2016]	[Kumar et al. 2022]	[Thakur et al. 2018]	[Thakur et al. 2019]	Proposed scheme
PSNR	44.5866	41.89231	50.4728	47.176	52.9137
NC	0.999852	0.997519	0.9997	0.999798	0.9991

Table 4: Comparison of PSNR and NC Values

Moreover, we have also evaluated the average of PSNR and NC with [Takore et al. 2016], [Kumar et al., 2022], [Thakur et al. 2018], and [Thakur et al. 2019]. The comparison of our results is tabulated in Table 4. The average PSNR value of the proposed scheme is 52.9137, whereas the PSNR values of [Takore et al. 2016], [Kumar et al., 2022], [Thakur et al. 2018] and [Thakur et al. 2019] are 44.5866, 41.8923, 50.4728, & 47.176 respectively. These values exhibit the good perceptual quality of the watermark images. Furthermore, the NC values of [Takore et al. 2016], [Kumar et al., 2022], [Thakur et al. 2018] and [Thakur et al. 2019] are 0.9998, 0.9975, 0.9997, & 0.9997 respectively whereas the proposed scheme has 0.9991. The comparison of PSNR and NC values from some of the existing schemes showed good perceptual quality of the medical image watermarking scheme. The above results have shown that the watermarked image could be recommended for diagnosis.

However, we will perform more experiments on different types of medical images such as X-ray images, MRI image, CT-scan image, mammography image, etc. so that our scheme would serve the medical field purposefully.

6   Conclusions

The present research work is based on FRT and Hessenberg decomposition watermarking approach. The recommended method is separated into two different stages. The first stage watermark insertion in which FRT is applied to the medical images. The transformed image is divided into blocks that do not overlap. The blocks of the host medical image are shuffled using a random number. After that, Hessenberg decomposition is employed, and the watermark is quantized into the host image. The obtained PSNR & NC value indicates the good performance of our scheme. The high PSNR value of the watermarked images resists to many attacks that we have obtained in our scheme. We have also obtained high SSIM values that show our scheme's better performance. Moreover, we have also assessed our scheme against some other existing schemes and found that the performance is better. We would like to further extend our work with video.

References

[Abd-Eldayem, 2013] Mohamed M. Abd-Eldayem.: "A proposed security technique based on watermarking and encryption for digital imaging and communications in medicine"; Egypt. Inform. J, 14, 1 (2013), 1–13.

[Ahmadi et al. 2021] Ahmadi, S. B. B., Zhang, G., Wei, S., Boukela, L.: "An intelligent and blind image watermarking scheme based on hybrid SVD transforms using human visual system characteristics"; The Visual Computer, 37,2 (2021), 385–409.

[Alzubi et al. 2011] Alzubi S, Islam N, Abbod M: "Multiresolution analysis using wavelet, ridgelet, and curvelet transforms for medical image segmentation"; Int J Biomed Imaging, Special Issue, (2011), 1–18.

[Araghi et al. 2018] Araghi, T. K., Abd Manaf, A., Araghi, S. K: "A secure blind discrete wavelet transform based watermarking scheme using two-level singular value decomposition"; Expert Systems with Applications, 112,1 (2018), 208–228.

[Araghi and Manaf 2019] Araghi, T. K., Abd Manaf, A.: "An enhanced hybrid image watermarking scheme for security of medical and non-medical images based on DWT and 2-D SVD"; Future Generation Computer Systems, 101, 1 (2019), 1223–1246.

[Ebrahimnejad and Naghsh 2021] Ebrahimnejad, J., and Naghsh, A.: "Adaptive Removal of high-density salt-and-pepper noise (ARSPN) for robust ROI detection used in watermarking of MRI images of the brain"; Computers in Biology and Medicine, 137,1 (2021), 104831–104840.

[Elhadad et al. 2021] Elhadad, A., Ghareeb, A., Abbas, S.: "A blind and high-capacity data hiding of DICOM medical images based on fuzzification concepts"; Alexandria Engineering Journal, 60, 2 (2021), 2471–2482.

[Fan et al. 2019] Fan, T. Y., Chao, H. C., Chieu, B. C.: "Lossless medical image watermarking method based on significant difference of cellular automata transform coefficient"; Signal Processing: Image Communication, 70, (2019), 174–183.

[Golub et al. 1979] Golub, G., Nash S., Loan C. V.: "A Hessenberg-Schur method for the problem AX + XB= C"; IEEE Transactions on Automatic Control, 24, 6, (1979), 909–913.

[Hou et al. 2019] Hou, J., Li, Q., Tan, R., Meng, S., Zhang, H., Zhang, S.: "An intrusion tracking watermarking scheme"; IEEE Access, 7,1 (2019), 141438–141455.

[Kumar et al. 2022] Kumar, A., Singh, K. U., Devadoss, V., Kant, T., Khader, A. Saudagar, A. K. J., Tameem A. A., Khathami, M. A., Khan, M. B., Hasanat, M. H. A., Malik, K. M.: "Robust Watermarking Scheme for NIfTI Medical Images"; CMC-Computers, Materials & Continua, 71, 2, (2022), 3107–3125.

[Liu et al. 2019] Liu, X., Lou, J., Fang, H., Chen, Y., Ouyang, P., Wang, Y., Wang, L.: "A novel robust reversible watermarking scheme for protecting authenticity and integrity of medical images"; IEEE Access, 7, 1 (2019), 76580–76598.

[Liu et al. 2018] Liu, Y., Tang, S., Liu, R., Zhang, L., Ma, Z.: "Secure and robust digital image watermarking scheme using logistic and RSA encryption"; Expert Systems with Applications, 97 (2018), 95–105.

[Liu et al. 2020] Liu, D., Yuan, Z., Su, Q.: "A blind color image watermarking scheme with variable steps based on Schur decomposition"; Multimedia Tools and Applications, 79, 11 (2020), 7491–7513.

[Malayil and Vedhanayagam 2021] Malayil, M. V., Vedhanayagam, M.: "A novel image scaling based reversible watermarking scheme for secure medical image transmission"; ISA transactions, 108 (2021), 269–281.

[Meenakshi et al.2020] Meenakshi, K., Swaraja, K., Kora, P.: "A hybrid matrix factorization technique to free the watermarking scheme from false positive and negative problems"; Multimedia Tools and Applications, 79, 39 (2020), 29865–29900.

[Molina-Garcia et al. 2020] Molina-Garcia, J., Garcia-Salgado, B. P., Ponomaryov, V., Reyes-Reyes, R., Sadovnychiy, S., Cruz-Ramos, C.: "An effective fragile watermarking scheme for color image tampering detection and self-recovery", Signal Processing: Image Communication, 81, (2020), 115725–115737.

[Najafi and Loukhaoukha 2019] Najafi, E., Loukhaoukha, K.: "Hybrid secure and robust image watermarking scheme based on SVD and sharp frequency localized contourlet transform"; Journal of information security and applications, 44 (2019), 144–156.

[Navamani et al. 2019] Navamani, T. M., Bharadwaj, A., Agrawal, R., Agarwal, U.: "Secure Transmission of DICOM Images by comparing different cryptographic algorithms"; Materials Today: Proceedings, 15 (2019), 1–11.

[Qasim et al. 2019] Qasim, A. F., Aspin, R., Meziane, F., Hogg, P.: "Assessment of perceptual distortion boundary through applying reversible watermarking to brain MR images"; Signal Processing: Image Communication, 70 (2019), 246–258.

[Rakhmawati et al. 2019] Rakhmawati, L., Wirawan, W., Suwadi, S.: "A recent survey of self-embedding fragile watermarking scheme for image authentication with recovery capability"; EURASIP Journal on Image and Video Processing, 61 (2019), 1–22.

[Sadreazami and Amini 2018] Sadreazami H., and Amini, M.: "A robust image watermarking scheme using local statistical distribution in the contourlet domain"; IEEE Transactions on Circuits and Systems II: Express Briefs, 66, 1 (2018), 151–155.

[Shehab et al. 2018] Shehab, A., Elhoseny, M., Muhammad, K., Sangaiah, A. K., Yang, P., Huang, H., & Hou, G.: "Secure and robust fragile watermarking scheme for medical images"; IEEE Access, 6 (2018), 10269–10278.

[Singh et al. 2022(a)] Singh, K. U., Hsieh, S. Y., Swarup, C., Singh, T.: "Authentication of NIfTI Neuroimages Using Lifting Wavelet Transform, Arnold Cat Map, Z-Transform, and Hessenberg Decomposition"; Traitement du Signal, 39, 1 (2022), 265–274.

[Singh et al. 2022(b)] Singh, K. U., Kumar, A., Singh, T., Ram, M.: "Image-based decision making for reliable and proper diagnosing in NIFTI format using watermarking"; Multimedia Tools and Applications, (2022), 1–27.

[Singh et al. 2022(c)] Singh, K. U., Abu-Hamatta, H. S., Kumar, A., Singhal, A., Rashid, M., Bashir, A. K.: "Secure watermarking scheme for color DICOM images in telemedicine applications"; Computers, Materials and Continua, 70, 2 (2022), 2525–2542.

[Singh et al. 2018] Singh, K. U., Singh, V. K., Singhal, A.: "Color image watermarking scheme based on QR factorization and DWT with compatibility analysis on different wavelet filters"; Journal of Advanced Research in Dynamical and Control Systems, 10, 06 (2018), 1796–1811.

[Singh and Singhal 2018] Singh, K. U., Singhal, A.: "Channelized noise augmentation to endorse DICOM medical image for diagnosing"; Journal of Advanced Research in Dynamical and Control Systems, 10, 06 (2018), 2228–2247.

[Takore et al. 2016] Takore, T., Kumar P. R., Devi G. L.: "A modified blind image watermarking scheme based on DWT, DCT and SVD domain using GA to optimize robustness," in 2016 Int. Conf. on Electrical, Electronics, and Optimization Techniques (ICEEOT), (2016), 2725–2729.

[Tan et al. 2019] Tan, Y., Qin, J., Xiang, X., Ma, W., Pan, W., Xiong, N. N.: "A robust watermarking scheme in YCbCrcolor space based on channel coding" IEEE Access, 7 (2019), 25026–25036.

[Thakur et al. 2018] Thakur, S., Singh, A. K., Ghrera, S. P., Mohan A.: "Chaotic based secure watermarking approach for medical images"; Multimedia Tools and Applications, 79 (2020), 4263–4276.

[Thakur et al. 2019] Thakur S, Singh A. K., Ghrera S. P., Elhoseny M.: "Multi-layer security of medical data through watermarking and chaotic encryption for tele-health applications"; Multimed Tools Appl, 78, 3 (2019), 3457–3470.

[Thanki et al. 2019] Thanki, R., Kothari, A., Trivedi, D.: "Hybrid and blind watermarking scheme in DCuT–RDWT domain"; Journal of Information Security and Applications, 46 (2019), 231–249.

[Wang et al. 2020] Wang, R., Shaocheng, H., Zhang, P., Yue, M., Cheng, Z., Zhang, Y.: "A novel zero-watermarking scheme based on variable parameter chaotic mapping in NSPD-DCT domain"; IEEE Access, 8 (2020), 182391–182411.

[Zainol et al. 2020] Zainol, Z., Teh, J. S., Alawida, M.: "A new chaotic image watermarking scheme based on SVD and IWT"; IEEE Access, 8 (2020), 43391–43406.

[Zheng and Zhang 2020] Zheng, P., and Zhang, Y.: "A robust image watermarking scheme in hybrid transform domains resisting to rotation attacks"; Multimedia Tools and Applications, 79, 25 (2020), 18343–18365.

[Zhong et al. 2020] Zhong, X., Huang, P. C., Mastorakis, S., Shih, F. Y.: "An automated and robust image watermarking scheme based on deep neural networks"; IEEE Transactions on Multimedia, 23 (2020), 1951–1961.